Vibrational spectroscopic studies and computational study of 5-chloro-N-(4,5-dihydro-1*H*-imidazol-2-yl)-2,1,3-benzothiadiazol-4-amine

N. R. Sheela*, S. Muthu and S. Sampath Krishnan

Department of Applied Physics, Sri Venkateswara College of Engineering, Sri Perumbudur, Tamil Nadu, India

_____

ABSTRACT

The solid phase Fourier transform infrared (FTIR) and Fourier transform (FT) Raman spectral analysis of 5-chloro-N-(4,5-dihydro-1H-imidazol-2-yl)-2,1,3-benzothiadiazol-4-amine (5CDIBTA) was carried out along with Restricted Hartree-Fock (RHF) and density functional theory (DFT) calculations (B3LYP) with the 6-31G (d, p) basis set. The thermodynamic functions of the above molecule were also performed using the RHF and DFT methods. Natural bond order analysis of the title molecule was also carried out. A detailed interpretation of the vibrational spectra of the compound has been made on the basis of the calculated potential energy distribution (PED). The calculated highest occupied molecular orbital (HOMO) and lowest unoccupied molecular orbital (LUMO) energies show that charge transfer occurs within the molecule. Comparison of the observed fundamental vibrational frequencies of the molecule and calculated results by RHF and DFT methods indicates that B3LYP is best fit for molecular vibrational problems. Comparison of the simulated spectra with the experimental spectra provides important information about the ability of the computational method to describe the vibration modes.

Keywords: RHF; DFT; FTIR; FT Raman; PED; Vibrational assignment; HOMO; LUMO.

_____

INTRODUCTION

The 5-chloro-N-(4, 5-dihydro-1H-imidazol-2-yl)-2, 1, 3-benzothiadiazol-4-amine (5CDIBTA) is α_2-adrenergic agonist and centrally active myotonolytic skeletal muscle relaxant with a chemical structure unrelated to other muscle relaxants [1]. It is in a class of medications called skeletal muscle relaxants, works by slowing action in the brain and nervous system to allow the muscle to relax owing to the presence of nitrate group in the structure. 5CDIBTA contains two hydrogen atoms in the cyclic guanidine moiety and exists as two tautomers [2].Various studies like

169

_____

spectrometric estimation and validation of 5CDIBTA [3] determination of 5CDIBTA in human plasma [4] was reported earlier.

To best of our knowledge, no theoretical Hartree Fock (HF) or density functional theory (DFT) calculations or detailed Vibrational infrared (IR) and Raman analysis have been performed on the title molecule. A detailed quantum chemical investigation will aid in understanding the Vibrational modes of 5CDIBTA and clarifying the experimental data available for this molecule. DFT calculations are known to provide excellent Vibrational wave numbers scaled to compensate for the approximate treatment of electron correlation, for basis set deficiencies and anharmonicity effects [5-10]. DFT is the best method rather than the ab initio method for the computation of molecular structure, Vibrational wavenumber and energies of molecule [11]. In this work by using the HF and B3LYP methods, we calculated the Vibrational wavenumbers of 5CDIBTA and molecular geometric parameters. These calculations are available for providing insight into the Vibrational spectra and molecular parameters.

MATERIALS AND METHODS

2.1. Experimental

The spectrometric pure sample of 5CDIBTA was procured from reputed pharmaceutical forms in Chennai, India and used as such without any further purification. The FTIR spectrum of the 5CDIBTA was recorded over the region 4000-400 cm^{-1} by using globar source adopting the KBr pellet technique at Sophisticated Analytical Instrumentation Facility (SAIF), IIT, Chennai. The FT-Raman spectrum was recorded on a Nexus 670 spectrometer at central Electro Chemical Research Institute Laboratory, Karaikudi, India. The laser frequency of 15,798 cm^{-1} was used as the excitation source. The spectrometer is fitted with an XT-KBr beam splitter and a DTGS detector. A base line correction was made for the spectrum recorded.
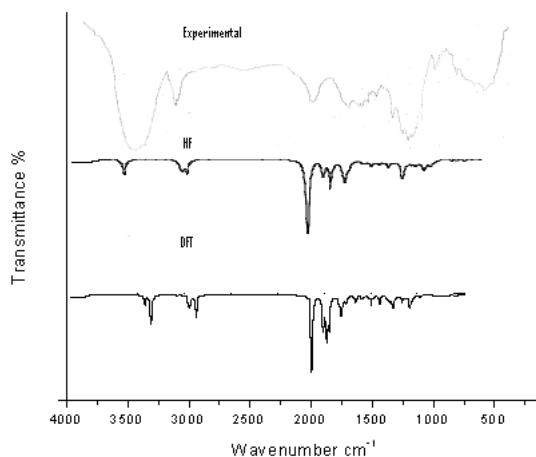

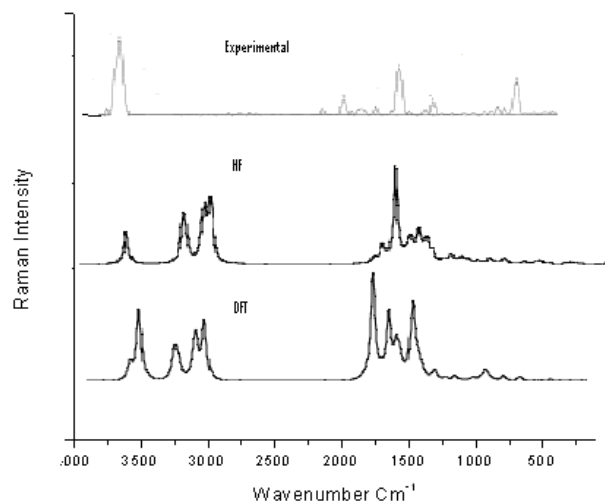**Fig. 1**. **Comparative representation of FTIR spectra for 5CDIBTA**

_____

Fig. 2. **Comparative representation of FT Raman spectra for 5CDIBTA**

The experimental and theoretically predicted FTIR and FT Raman spectra of 5CDIBTA with their scaled frequencies using scaled factors for each mode are respectively shown in Figs. 1 and 2 for comparison.

2.2. Computational Details.

The entire calculations were performed at RHF and B3LYP levels on a Pentium iv/1.6GHZ personal computer using the Gaussian 03W program package [12]. The geometries first optimized at the RHF level of theory employing the 6-31G(d, p) basis set. DFT employed the B3LYP keyword which invokes Becker's three parameter hybrid method [11] using the correlation function of Lee et al [13]. The optimized structural parameters were used in the Vibrational frequency calculations to characterize all stationary points as minima. DFT offers electron correlation which is frequently comparable to second order Moller-plesset theory MP2 [14, 15] vibrational frequencies. To compensate errors arising from the basis set in completeness and neglect of Vibrational anharmonicity we have scaled the frequencies with scaling factor, 0.903(HF) [16] and 0.961(B3LYP) [17]. Next the spectrum was analyzed in terms of the PED contribution by using the VEDA program [18]. Finally, the calculated normal mode Vibrational frequencies also provide the thermodynamic properties through the principle of statistical mechanics. The assignments of the calculated wavenumbers supported by the animation option of chemcraft a graphical interface for Gaussian programmes, which gives a visual presentation of the shape of the Vibrational modes [19].

RESULTS AND DISCUSSION

3.1. Molecular geometry

The optimized molecular structure for 5CDIBTA in the ground state was computed by the RHF and B3LYP calculations computed by the 6-31G (d, p) basis set. The values of the total energy for 5CDIBTA from the RHF and B3LYP calculation by employing the 6-31G9d,p) basis set are found to be –1474.6813a.u and –1479.9041a.u, respectively. The calculated geometrical

_____

parameters (bond lengths and bond angles) were compared with experimentally obtained x-ray diffraction (XRD) data values [20]. As the experimental values for 5CDIBTA are known, the theoretically calculated values may give an idea about the geometry of the molecule changes from the ab initio method of calculation and the DFT method of calculation. The optimized structural parameters of 5CDIBTA from the RHF/6-31G (d ,p) and B3lYP/6-31G (d, p) calculations and the XRD values are listed in Table 1, in accordance with the atom numbering scheme given in Fig. 3. The slight deviation in XRD data from the computed geometry is probably due to the fact that the intermolecular interactions in the crystalline state are dominant. The B3LYP method leads to geometry parameters, which are close to experimental data [20]. A statistical treatment of these data shows that, for the bond lengths, B3LYP/6-31G (d, p) is better than the RHF/6-31G (d, p) geometry.

Table 1.Optimized parameters of 5CDIBTA at B3LYP and RHF with 6-31G(d,p) basis set

| Bond length(Å)				Bond angle(°)			
	HF	DFT	Reference		RHF	DFT	Reference
N1-S2	1.62	1.647	1.2924	S2-N1-C5	108	107	117.8
N1-C5	1.3	1.337	1.26	N1-S2-N3	98.4	99.6	96.2
S2-N3	1.616	1.639	1.696	N1-C5-C4	112.7	113	111.0
N3-C4	1.3	1.338	1.26	N1-C5-C9	126.4	126	129.0
C4-C5	1.442	1.456	1.337	S2-N3-C4	108	106.9	104.0
C4-C6	1.435	1.421	1.337	N3-C4-C5	112.9	113.4	111.0
C5-C9	1.452	1.445	1.337	N3-C4-C6	126.8	125.6	129.0
C6-C7	1.339	1.368	1.337	C5-C4-C6	120.3	121	120.0
C6-H17	1.073	1.083	1.1	C4-C5-C9	120.9	120.9	120.0
C7-C8	1.449	1.424	1.3372	C4-C6-C7	117.5	117.3	120.0
C7-H18	1.073	1.084	1.1	C4-C6-H17	120	120.3	120.0
C8-C9	1.35	1.392	1.337	C5-C9-C8	115.4	114.7	120.0
C8-Cl16	1.739	1.759	1.719	C5-C9-N10	120.9	124.3	120.0
C9-N10	1.398	1.385	1.266	C7-C6-H17	122.5	122.4	120.0
N10-C11	1.385	1.395	1.266	C6-C7-C8	122.1	121.9	120.0
N10-H19	0.997	1.013	1.05	C6-C7-H18	120.8	120.5	120.0
C11-N12	1.259	1.287	1.26	C8-C7-H18	117.1	117.5	120.0
C11-N15	1.38	1.388	1.266	C7-C8-C9	123.8	124.2	120.0
N12-C13	1.455	1.468	1.47	C7-C8-Cl16	115.6	116.6	120.0
C13-C14	1.546	1.553	1.15	C9-C8-Cl16	120.5	119.3	120.0
C13-H20	1.087	1.095	1.113	C8-C9-N10	123.4	120.8	120.0
C13-H21	1.084	1.099	1.113	C9-N10-C11	125.6	132.3	120.0
C14-N15	1.462	1.474	1.47	C9-N10-H19	114.3	114.5	120.0
C14-H22	1.083	1.099	1.113	C11-N10-H19	109.6	109.4	120.0
C14-H23	1.087	1.094	1.113	N10-C11-N12	121.2	119	124.5
N15-H24	0.996	1.016	1.05	N10-C11-N15	120.8	122.7	124.5
r	0.8405	0.8486		N12-C11-N15	118	118.2	111.0
				C11-N12-C13	106.7	105.5	104.0
				C11-N15-C14	105.1	104.7	108.0
				C11-N15-H24	115.4	115.4	126.0
				N12-C13-C14	105.3	105.7	112.3
				N12-C13-H20	109.6	111.1	108.7
				N12-C13-H21	111.1	109.5	107.8
				C14-C13-H20	111.2	112.5	108.7
				C14-C13-H21	112.3	110.9	107.8
				C13-C14-N15	101.6	101.4	104.7
				C13-C14-H22	113.3	111.5	110.6
				C13-C14-H23	111.5	113.3	112.2
				H20-C13-H21	107.3	107.1	111.4
				N15-C14-H22	111.2	111.1	110.6
				N15-C14-H23	110.8	111.2	112.2
				C14-N15-H24	116.6	117.1	126.0
				H22-C14-H23	108.3	108.3	106.5
				r	0.8209	0.7925	

_____
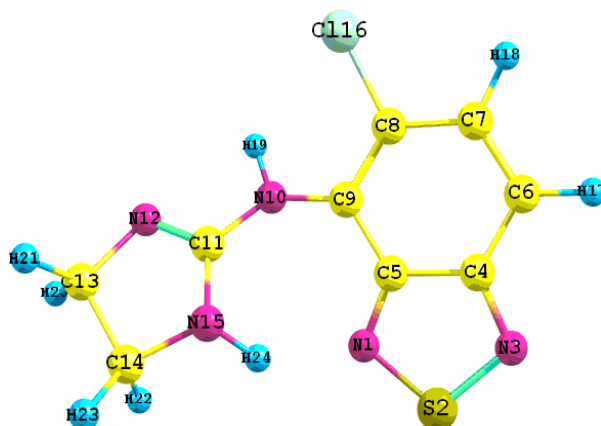
Fig.3.Numbering system adopted in the molecular Structure of 5CDIBTA

The correlation Coefficient (r) for bond lengths computed from the DFT and RHF methods with the experimental values were found to be 0.8482 and 0.8409, respectively. Similarly, the 'r' for bond angles computed from the DFT and RHF methods with the experimental values were found to be 0.7925 and 0.8209, respectively. It can be noted from the 'r' values that the theoretical predictions are not in good agreement with the experimental value for bond angles.

3.2. Natural population Analysis

The calculation of effective atomic charges plays an important role in the application of quantum mechanical calculations to molecular systems. Our interest here is in the comparison of different method (RHF and DFT) to describe the electron distribution in 5CDIBTA as broadly as possible, and to assess the sensitivity of the calculated charges to changes in the choice of the quantum chemical method. The calculated natural atomic charge values from the natural population analysis (NPA) and Mulliken population analysis (MPA) procedures using the RHF and DFT methods are listed in Table 2.The NPA from the natural bonding orbital (NBO) method is better than the MPA scheme. Table 2, compares the atomic charge site of 5CDIBTA from both MPA and NPA methods. The NPA of 5CDIBTA shows that the presence of two active hydrogen atoms in the guanidine moiety [H_{19}=0.46711(RHF) and 0.45240(DFT).H_{24}=0.53149 (RHF) and 0.48466 (DFT)] due to less negative charges on nitrogen atoms [N_{10}=-0.69182 (RHF) and –0.59642 (DFT),N_{15}=-0.92513 (RHF) and –0.71719 (DFT)]. Moreover there is no difference in charge distribution observed on all other hydrogen atoms. The large negative charges on N_{15}, N_{10} and N_{12} possess the less positive charges on the carbon atoms C_{14} and C_{13} are almost same and negative. Also, the NPA of 5CDIBTA shows the presence of two nitrogen atoms in the Imidozoline ring [N_1=-0.7348(RHF) and –0.68816 (DFT), N_3=-0.63936 (RHF) and –0.63232 (DFT) and less positive charges on the carbon atoms C_5 and C_4, respectively. The charge possessed by the carbon atoms C_8 is less negative due to the positive charge accumulated on the C_{16} atom.

173

_____

Table 2. Natural atomic charges of 5CDIBTA

Atom with Numbering	MPA		NPA	
	HF	DFT	HF	DFT
1 N $_1$	-0.710	-0.601	-0.734	-0.688
2 S $_2$	0.802	0.641	1.084	0.994
3 N $_3$	-0.554	-0.526	-0.639	-0.632
4 C $_4$	0.198	0.210	0.174	0.147
5 C $_5$	0.297	0.288	0.225	0.156
6 C $_6$	-0.148	-0.084	-0.300	-0.280
7 C $_7$	-0.082	-0.074	-0.174	-0.216
8 C $_8$	-0.275	-0.199	-0.128	-0.108
9 C $_9$	0.535	0.450	0.243	0.171
10 N $_{10}$	-0.897	-0.696	-0.692	-0.596
11 C $_{11}$	0.856	0.638	0.742	0.567
12 N $_{12}$	-0.694	-0.538	-0.762	-0.617
13 C $_{13}$	-0.017	-0.054	-0.222	-0.280
14 C $_{14}$	-0.004	-0.054	-0.219	-0.282
15 N $_{15}$	-0.900	-0.631	-0.925	-0.717
16 Cl$_{16}$	0.057	0.031	0.030	0.046
17 H $_{17}$	0.201	0.119	0.268	0.267
18 H $_{18}$	0.207	0.128	0.271	0.269
19 H $_{19}$	0.362	0.292	0.467	0.453
20 H $_{20}$	0.084	0.083	0.193	0.216
21 H $_{21}$	0.083	0.083	0.192	0.215
22 H $_{22}$	0.076	0.084	0.186	0.216
23 H $_{23}$	0.078	0.084	0.188	0.217
24 H $_{24}$	0.443	0.328	0.531	0.485

3.3.Vibrational assignments.
According to the theoretical calculations, 5CDIBTA has a structure of C_1 point group symmetry. The molecule has 24 atoms and 66 modes of fundamental vibrations.
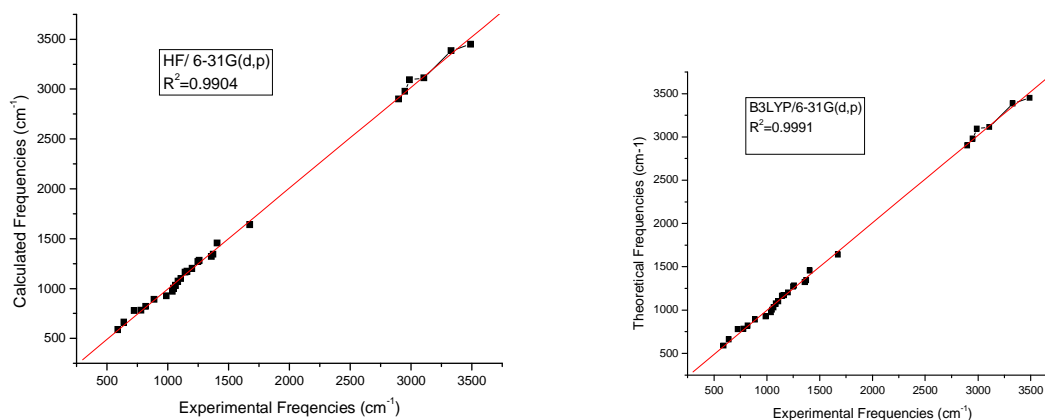

Fig. 4. Graphic correlation between the experimental and calculated wavenumber obtained by the *ab-initio* HF and DFT methods for 5CDIBTA

_____

Table 3. Comparison of the calculated and experimental wavenumbers (cm⁻¹) and intensities (km/mol) of 5CDIBTA

| Mode Nos. | Observed wavenumbers (cm⁻¹) | | Calculated wavenumbers (cm⁻¹) | | | | | | | | Vibrational Assignments (PED) |
| | FTIR | FT -Raman | RHF/6-31G(d,p) | | | | B3LYP/6-31G(d,p) | | | | % |
			Unscaled frequency	Scaled frequency	IR Intensity	Raman Intensity	Unscaled frequency	Scaled frequency	IR Intensity	Raman Intensity	
1	3490 (w)	-	3854	3480	12.21	25.14	3590	3450	13.14	15.26	ν_{as} NH (100)
2	3330(w)	-	3850	3477	9.30	9.72	3522	3385	36.90	66.12	ν_{as} NH(98)
3	3107(m)	-	3405	3074	0.39	44.79	3240	3114	0.21	27.04	Aromatic CH asym(77)
4	2990(m)	-	3385	3057	0.22	15.60	3219	3094	0.38	12.15	Aromatic CH asym(75)
5	2950	2950(m)	3257	2941	9.39	27.97	3098	2978	10.52	18.62	ν_{as} CH$_2$(69)
6	-	2887(vs)	3234	2920	9.63	42.83	3079	2959	13.25	32.25	ν_{as} CH$_2$(67)
7	2899(w)	-	3190	2881	11.32	45.59	3019	2901	16.79	31.44	ν CH$_2$(58)
8	-	-	3184	2876	7.83	15.88	3013	2896	13.27	23.01	NH deformation(74)
9	1675(vs)	1675(w)	1902	1717	100.00	6.79	1708	1641	100.00	99.97	Ring C-C stretching vibration(53)
10	-	-	1840	1662	0.02	17.61	1639	1575	1.49	6.92	Ring C-C stretching vibration(51)
11	-	-	1739	1570	15.55	100.00	1581	1519	43.53	58.66	δ CH$_2$ (82)
12	-	-	1735	1567	4.48	0.50	1550	1489	37.37	1.56	C…C stretching of pyridine ring(74)
13	-	-	1672	1510	5.51	2.70	1540	1480	21.82	2.51	δ CH$_2$ (81)
14	-	1466(s)	1654	1493	28.60	4.82	1520	1461	14.64	25.65	δ CH$_2$ (79)
15	1407(m)	1407(m)	1643	1483	7.45	4.22	1515	1456	25.26	1.22	δ CH$_2$ (74)
16	-	-	1620	1463	0.82	20.22	1494	1436	6.52	14.18	τ CNCN
17	-	-	1565	1413	2.75	29.85	1417	1362	5.69	6.07	τ ClCCN
18	1375(m)	-	1527	1379	4.89	8.88	1400	1346	9.36	64.51	τ CCCCl
19	1360(m)	-	1502	1356	19.60	1.82	1375	1322	22.75	3.19	τ CCCN
20	-	-	1494	1349	7.68	19.48	1359	1306	6.60	11.68	ν CN (52)
21	-	-	1468	1325	2.68	3.08	1343	1291	2.15	0.71	w CH$_2$ (31) / β CH (69)
22	1260(m)	-	1451	1310	5.74	3.75	1334	1282	1.73	4.07	β CH deformation(47)
23	1250(m)	1250(w)	1438	1298	3.77	3.50	1321	1270	9.62	2.90	w CH$_2$ (58)
24	1200(m)	-	1360	1228	0.08	2.10	1250	1201	0.12	1.53	w CH$_2$ (66)
25	1160(s)	-	1321	1193	1.12	2.21	1221	1173	9.47	6.21	β CH deformation(72)
26	1145(w)	-	1299	1173	4.49	8.85	1212	1165	1.61	1.72	t CH$_2$ (35)
27	1109(vw)	1109(vs)	1233	1113	4.98	3.10	1145	1100	4.58	1.13	β CH deformation(74)
28	-	1050(w)	1220	1102	0.70	0.10	1140	1096	1.84	1.10	β CH deformation(49)
29	1085(w)	-	1213	1095	5.09	5.74	1117	1074	1.17	0.19	w CH$_2$ (63)
30	1065(w)	-	1167	1053	2.58	3.07	1074	1032	1.85	3.72	ν C-N-C (55)
31	1050(vw)	-	1140	1030	5.57	0.34	1044	1003	12.84	0.86	ν C-C-N (69)

175

_____

32	1040(w)	-	1111	1003	0.01	0.89	1012	972	2.28	0.69	γ CH deformation(76)
33	990(s)	-	1092	986	0.96	2.33	965	927	0.05	0.16	γ CH deformation(37)/SN (27)
34	-	975(w)	1047	946	10.16	1.71	950	913	12.08	0.86	γ CH deformation(39)
35	889(m)	889(w)	995	898	1.07	4.60	929	892	1.26	2.08	ρ CH$_2$(45) /HCCH deformation(32)
36	-	865(w)	966	872	3.50	1.29	878	843	0.13	2.88	ρ CH$_2$(27) / ν C-N (41)
37	820(m)	-	888	849	9.92	0.97	854	821	5.86	0.87	γ CH(42) /NSN deformation(33)
38	-	800(m)	888	822	4.33	1.79	836	804	7.49	6.51	SNC deformation (21)
39	780(s)	-	875	815	9.26	1.80	816	784	2.66	3.97	w NH (72)
40	725(s)	-	875	802	9.92	0.97	812	780	6.03	0.27	w NH (67)
41	-	-	868	790	4.33	1.79	790	759	14.05	1.36	ρ CH$_2$ (39)
42	-	-	868	784	9.26	1.80	777	747	2.57	0.45	CN bending vibration(44)
43	-	700(w)	827	747	3.18	0.56	750	720	1.37	0.52	γ CH /CC ring breathing(51)
44	-	655(w)	786	710	5.20	0.83	695	668	7.80	1.34	ρ CH$_2$(67)
45	640(m)	-	747	675	4.90	0.89	690	663	3.90	2.99	γ CH(62)
46	-	-	729	658	3.25	1.62	667	641	1.24	0.69	w NH(59) / β NCN(23)
47	-	-	691	624	4.11	0.99	642	617	3.63	0.20	γCH(37)/ β NCN(57)
48	590(m)	-	656	593	8.94	0.52	613	589	15.83	0.15	β CCC(44)
49	-	570(w)	639	577	5.65	1.45	584	561	7.78	0.74	γ CH(72)
50	-	-	603	545	2.60	2.85	575	553	1.96	0.60	γ CCNH
51	-	525(w)	584	527	6.64	1.09	561	540	2.34	3.16	β NCC(63)
52	-	475(w)	545	492	1.52	0.29	497	478	2.04	0.22	β CCC(39)/ ν CCl(41)
53	-	-	524	473	0.23	0.59	481	462	0.68	0.22	C-C-N asym deformation (57)
54	-	357(vs)	404	365	0.13	0.78	378	364	0.19	1.09	C-C-N sym deformation(51)/ γ NCN(29)
55	-	-	367	332	0.93	1.43	329	316	0.18	0.48	β C-C-Cl(68)
56	-	-	362	327	0.11	1.09	325	312	1.23	1.57	β CH(70)
57	-	-	313	283	0.90	0.75	276	265	1.17	1.17	CCN deformation(45)
58	-	-	269	243	0.34	0.48	254	244	0.86	0.16	γ CCl(61)
59	-	-	240	216	0.65	0.11	226	217	1.26	0.13	γ CH$_2$(68)
60	-	-	221	200	0.70	0.11	210	202	1.00	0.15	γ CH$_2$(71)
61	-	-	200	181	0.12	0.35	198	190	0.33	0.54	γ C-C-Cl (44)/ γ CNH(28)
62	-	-	157	141	0.84	0.05	171	165	1.06	0.07	t CH$_2$
63	-	119(vw)	105	95	0.10	0.25	110	106	0.24	0.18	CH$_2$. CH$_2$ See Saw (55)+ γ C-Cl(31)
64	-	-	74	67	0.05	0.55	76	73	0.01	0.29	Cl CCN bending(29)
65	-	-	54	49	0.45	0.25	54	51	0.99	0.15	γ CH$_2$(63)
66	-	-	46	42	0.14	1.64	39	38	0.24	0.99	γ CH$_2$(59)

_____

Inclusion of electron correlation in DFT to a certain extent makes the frequency values smaller in comparison with the HF frequency data. For the plots of simulated IR and Raman spectra, pure Lorentzian band shapes were used with a bandwidth of 40 cm^{-1}. Figs 1 and 2 show comparative representation of theoretical and experimental FTIR and FT Raman spectra respectively.

It should be noted that Gaussian 03W package does not calculate the Raman intensities. The Raman activities were transformed into Raman intensities, using Raint program [22] by the expression.

$$I_i = 10^{-12} (v_{0-} v_i)^4 (I/ v_i) Si$$

Where I_i is the Raman intensity, S_i is the Raman scattering activities, v_i is the wave number of normal modes, and $v0$ denotes the wave number of the excitation laser [23].

3.3.1. *NH vibrations*
The vibrations belonging to N-H stretching [24] occur in the region 3500-3400cm^{-1}. In the present work the bands observed at 3500 cm^{-1} and 3320 cm^{-1} in FTIR spectrum (mode no 1) have been assigned to asymmetric and symmetric vibrations of NH group respectively. This is also in very good agreement with the computed value. N-H bending is usually observed in the region 1650-1515 cm^{-1}, which is called the amide band [25]. In the present work the band appeared at 1675 cm^{-1} in FTIR and FT Raman spectra is assigned to NH deformation vibration (mode no 9) and are comparable with the theoretical values. The N-H wagging vibration [24] occurs at 780 and 725 cm^{-1} in FTIR and FT Raman spectra (mode no 39, 40) and NH out-of - plane bending occurs at 641 cm^{-1} by B3LYP/6-31G (d, p) method (mode no 46). These are well comparable with the literature values and are presented in Table 3.

3.3.2. *Methylene group of vibrations*
Methylene C-H stretching vibrations occur generally in the region of 3000-2840 cm^{-1} [24]. C-H stretching vibrations are the most stable in the spectrum. In the present work the asymmetric stretching vibration occurs at 2950 cm^{-1} in FTIR and at 2950 and 2887 cm^{-1} in FT Raman spectra, (mode no 5,6). The symmetric stretching vibration occurs at 2880 cm^{-1} in FTIR spectrum (mode no 7). The theoretically computed values of CH_2 asymmetric stretching gives wave number at 2895 cm^{-1} by B3LYP/6-31G (d, p) method (mode no 8) coincides exactly with literature data. The bending vibrations of CH bonds in the methylene group are referred to as scissoring, rocking, twisting and wagging. The scissoring band in the spectra of hydrocarbons occurs at a constant position near 1465 cm^{-1} [26]. The absorption of hydrocarbons, due to methylene twisting and wagging is observed in the region 1350-1150 cm^{-1}[26,27]. The band resulting from the methylene rocking vibration in which all of methylene groups rock in phase appear at 720 cm^{-1} [27]. In the present work scissoring occurs at 1466 cm^{-1} in FT Raman spectrum and at 1407 cm^{-1} in FTIR and FT Raman spectra, rocking vibration occurs at 889 cm^{-1} in FTIR and at 889,865 and 655 cm^{-1} in FT Raman spectra, wagging vibrations at 1250, 1085 cm^{-1} in FTIR and at 1250 cm^{-1} in FT Raman spectra and twisting vibrations due to CH_2 group at 1145 cm^{-1} in FTIR spectrum are presented in Table 3. These are well comparable with theoretically calculated values. The remaining vibrations are assigned and are presented in the Table 3.

_____

3.3.3. C-H vibrations

Most mononuclear and polynuclear compounds have three or four peaks in the region 3100-3010 cm^{-1}, these being due to stretching vibrations of the ring C-H bands [28]. In the present work the FTIR bands at 3107 and 2988 cm^{-1} have been assigned to aromatic C-H stretching vibrations. Bands of variable intensity are observed in the regions 1300-1180 cm^{-1} region are due to in plane deformation vibrations, while those appearing in the region 900-650 cm^{-1},characteristic of the position of the substituents are due to the C-H out of plane vibrations [29,30]. The frequencies at 1260,1160 and 1109 cm^{-1} in FTIR and at 1109 and 1050 cm^{-1} in FT Raman spectra have been assigned to C-H in plane deformation vibrations (mode no 22,25,27,28). Bands observed at 1040,990,640 and 590 cm^{-1} in FTIR and at 975,820,700 and 570 cm^{-1} (mode nos 34,43 and 49) in FT Raman spectra have been assigned to out of plane C-H bending vibrations and are in good agreement with the theoretical values.

3.3.4. Pyridine Vibrations

The correlation of the absorption bands of simple compounds with their structure can provide a means for determining the structure of more complex compounds. The most of the previous works [31, 32] are examined to indicate general applicability of correlations. Young, Durall and Wright [33] presented absorption patterns for benzene in the 1600-2000 cm^{-1} region that are typical with respect to the position and number of substituted groups. It has been suggested that many of the vibrations are quite close to those of benzenes. Therefore, similar correlations are expected to exist for the pyridine also.

3.3.5. C-N and C-C vibrations

Aromatic amines normally display a strong stretching absorption in the region 1342-1266 cm^{-1} [33]. These absorptions occur at higher frequencies than the corresponding absorptions in amines as the force constant of the C-N bond is increased by resonance with the ring. In the present work the wave numbers calculated by B3LYP/6-31G (d, p) at 1306 cm^{-1} (mode no 20) and 747 cm^{-1} (mode no 42) assigned to C-N stretching and bending vibrations, respectively. The stretching vibration of C-N-C [34] is identified at 1065 cm^{-1} in FTIR spectrum (mode no 30) and is in good agreement with the theoretically computed values. The band observed at 1050 cm^{-1} in FTIR spectrum is assigned to C-C-N stretching vibrations (mode no 31) which is in good agreement with the theoretically computed values. The theoretically computed values of C-N-C deformations falls at 462,365 and 265 cm^{-1} (mode nos 53, 54 and 57) and are found to be in good agreement with the experimental data. The band observed at 525 cm^{-1} in FT Raman spectrum has been assigned to N-C-C bending vibration, is also in good agreement with the theoretical value (mode no 51). The ring carbon-carbon stretching vibrations generally occur in the region 1625-1430 cm^{-1} (25, 26). Accordingly the wavenumbers calculated by the B3LYP/6-31G (d, p) method for C-C stretching vibration identified at 1575, 1519 and 1480 cm^{-1} (mode nos 10,11 and 13). The theoretically calculated C-C-C bending vibrations have been found to be consistent with the recorded spectral values and are listed in the Table 3. The remaining vibrations are assigned and are presented in the Table 3.

3.3.6 N-C-N and S-N vibrations

The N-C-N in plane bending vibration contributes mainly to the normal modes (DFT mode nos 10, 11 and 13) at 641 and 617 cm^{-1} is almost coincides with experimental value. This assignment is also find support from literature value [35]. In our title molecule the band observed at 357 cm^{-1}

_____

in FT Raman spectrum (mode no 54) is assigned to N-C-N out of plane bending which is in good agreement with the theoretically computed value. The S-N stretching vibrations exhibits in the region 1010-1020 cm^{-1}[36], the band observed at this region is not pure stretching S-N vibration and contains a significant contribution of out of plane bending CH mode .In the present work band observed at 990 cm^{-1} in FTIR spectrum is assigned to S-N stretching vibration (mode no 33) which is in good agreement with the theoretically computed value.

3.3.7 C-Cl vibrations

The vibrations belonging to the bond between the ring and the halogen atoms are worth to discuss here, since mixing of vibrations are possible due to the lowering of the molecular symmetry and the presence of heavy atoms on the periphery of molecule [37]. The assignments of C-Cl stretching and deformation vibrations have been made by comparison with similar molecules p-bromo phenol [38] and the halogen substituted benzene derivatives [39]. Mooney [40, 41] assigned vibrations of C-X group (X=Cl, Br and I) in the frequency range of 1129-480 cm^{-1}. The C-Cl stretching vibrations give generally strong bands in the region 710-505 cm^{-1}. From the above literature value the band observed at 475 cm^{-1} in FTIR spectrum is assigned to C-Cl stretching vibration (mode no 52). Krishna Kumar et al [42] assigned the C-Cl in plane and out of plane bending vibration at 263 and 229 cm^{-1} in FTIR spectrum, our present study the computed wave numbers at 316 cm^{-1} and 244,190 and 106 cm^{-1} (mode nos 55,58 and 61) are assigned to C-Cl in-plane and out-of plane bending vibrations respectively.

Table 4. Theoretically computed energies(a.u),Zero-point Vibrational energies(kcal mol^{-1})Rotational constants (Ghz),Entropies(cal mol^{-1}k^{-1}),Dipole moment (D) Heat capacity (kcal mol^{-1} k^{-1}) and Rotational temperature(Kelvin) of 5CDIBTA

Parameters	HF/6-31G(d,p)	B3LYP/6-31G(d,p)
Total energy	-1474.6813	-1479.9041
Zero point energy	117.65757	108.79146
Rotationa Constants	0.54763	0.52099
	0.38406	0.38406
	0.38406	0.22719
Entropy		
Total	46.020	49.748
Translational	2.981	2.981
Rotational	2.981	2.981
Vibrational	40.058	40.058
Electronic	0.000	0.000
Dipole moment	2.6862	2.4073
Rotational Temperature	0.02628	0.02500
	0.01843	0.01851
	0.01139	0.01090

3.4. Thermodynamic properties

Entropy of the title compound is presented in Table 4. Scale factors have been recommended [43] for an accurate prediction in determining the ZPVE and the entropy. The variation in the ZPVE's seem to be insignificant. The total energies and the changes in the total entropy of the 5CDIBTA at room temperature at different methods are also presented. Dipole moment is a measure of the asymmetry in the molecular charge distribution and is given as a vector in the three dimensions. The values of dipole moments and energies for the title molecule were also

_____

calculated and listed in the Table 4. According to HF and DFT (B3LYP) calculations, the largest dipole moment and the lowest energy were observed for B3LYP/6-31G (d, p).

3.5. HOMO and LUMO analysis

Many organic molecules, containing conjugated л electrons are characterized by large values of molecular first hyperpolarizabilities, were analyzed by means of vibrational spectroscopy [44,45]. In most cases, even in the absence of inversion symmetry, the strongest bands in the Raman spectrum were weak in the IR spectrum and vice versa. But the intermolecular charge transfer from the donor to acceptor group through a single-double bond conjugated path can induce large variations of both the molecular dipole moment and the molecular polarizability, making IR and Raman activity strong at the same time. The experimental spectroscopic behavior described above is well accounted for ab initio calculations in л conjugated systems that predict exceptionally large Raman and infrared intensities for the some normal modes [46]. It is also observed in our title molecule the bands in FTIR spectrum have their counter parts in Raman shows that the relative intensities in IR and Raman spectra are comparable resulting from the electron cloud movement through л conjugated frame work from electron donor to electron acceptor groups. The analysis of the wave function indicates that the electron absorption corresponds to the transition from the ground to the first excited state and is mainly described by one-electron excitation from the HOMO to the LUMO. The LUMO of л nature, (i.e., heterocyclic ring) is delocalized over the whole C-C and C-N bond.

Since,DFT based chemical reactivity description provides valuable information about the reactive sites for various types of attacks and orientation for benzidene [47]**,** we have applied the same concepts during the studies. The Mulliken electronegativity (χ) [48],chemical hardness (η) and electronic potential were computed using orbital energies of the HOMO and the LUMO at the B3LYP/6-31G(d,p) and HF/6-31G(d,p) levels of theory. The ionization potential (μ) of the molecule is calculated using Koopman's theorem[49] and is given by

$$\mu = (E_{Homo} + E_{Lumo}) / 2$$

using Koopman's theorem, chemical hardness is calculated using,

$$\eta = (E_{Lumo} - E_{Homo}) / 2$$

Considering the chemical hardness, large Homo-Lumo gap means a hard molecule and small Homo-Lumo gap means a soft molecule [50].One can also relate the stability of the molecule to hardness, which means that the molecule with least HOMO-LUMO gap means it is more reactive.

The HOMO-LUMO energy of the 5CDIBTA was calculated at the B3LYP/6-31G (d, p) level and are shown in Fig. 5, which reveals that the energy gap reflect the chemical activity of the molecule. LUMO as an electron acceptor represents the ability to obtain an electron, HOMO represents the ability to donate an electron. The energy gap of the 5CDIBTA was calculated and tabulated in the Table 5.In general, the HOMO becomes less bound while the LUMO becomes more bound.From Table 5, it is concluded that the lowest energy gap was found at the DFT method. The atomic orbital compositions of the molecular orbitals are sketched in Fig. 5.
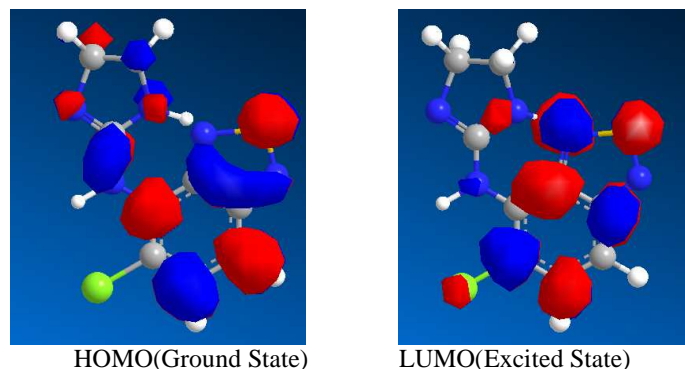
_____

HOMO(Ground State)   LUMO(Excited State)

Fig. 5. The atomic orbital compositions of the frontier molecular orbital for 5CDIBTA

HOMO Energy (E_{Homo}) = 5.532118 a.u
LUMO Energy (E_{Lumo}) = -2.731773 a.u
HOMO-LUMO (Energy gap) = 2.800346 a.u

Table 5. Comparison of HOMO,LUMO, Energy gaps and Ionization potentials of 5CDIBTA

Basis set	HF/6-31G(d,p)	B3LYP/6-31G9d,p)
E_{homo}	-8.609478	-5.532118
E_{lumo}	0.766279	-2.731773
Chemical Hardness (η)	4.68787	1.40016
Ionisation Energy (μ)	-3.92159	-4.13194
Energy gap	9.375757	2.800346
Electronegativity(χ)	-4.68787	-1.40016

The calculated self-consistent field (SCF) energy of 5CDIBT is -1479.90418954 a.u. In addition, the decrease in the HOMO and LUMO energy gap explains the eventual charge transfer interaction taking place within the molecule which is responsible for the chemical activity of the molecule.

CONCLUSION

The detailed interpretation of the vibrational spectra of the title molecule has been performed based on the quantum mechanical approach by the RHF and B3LYP method using Gaussian program. The fitting between calculated and measured vibrational frequencies was achieved by these methods and the deviation between calculated and experimental values is quite small after scaling frequencies. Therefore this study confirms that the theoretical calculation of the vibrational frequencies for the 5CDIBTA is quite useful for determining the vibrational assignment and for predicting new vibrational frequencies. The theoretically calculated values of both bond lengths and bond angles of the structures of the minimum energy were then compared with X-ray crystallographic data. The data obtained during the course of present investigation show that better agreement between the experimental and computed data is obtained using the DFT method B3LYP with the basis set 6-31G (d, p).

The lowering of the HOMO-LUMO energy gap value has substantial influence on the intramolecular charge transfer and bioactivity of the molecule.The bond order and atomic charges of the title molecule have been studied by both RHF and DFT method. The calculated

181

_____

normal mode vibrational frequencies provide thermodynamical properties by way of statistical mechanics.

REFERENCES

[1] TSe FLS, Jaffe Jm and Bhuta S, *Fundam clin pharmacol*,**1987,** 1**,** 479.

[2] L.J.Jackman and T.Jen, *J.Am.Chem.Soc,***1975,** 97, 2818.

[3] R. Siva Kumar et.all, *Int.J.Pharm tech Research*,**2010**, 2, 949.

[4] Dong-Hyun kim et. all, mass spectrometry, *Analyst*,**2002,** 127, 920.

[5] N.C.Handy, C.W.Murray and R.D.Amos, *J.phys.Chem*.,**1993,** 97, 4396.

[6] O.J.Stephens, F.J.Devlin, C.F.Chavalowski, and M.J.Frisch.*J.Phys.Chem*.,**1994,** 98,11627

[7] F.J.Devlin.J.W.Finley, P.J.Stephens, and M.J.Frisch, *J.phys.chem*.,**1995,** 99, 16902

[8] S.Y.Lee and B.H.Boo, Bull.Korean*, Chem.soc*.,**1996,** 17, 759.

[9] S.Y.Lee and B.H.Boo,**1996**, 17,764.

[10] G.Rahnut and P.Pulay, .*J.Phys, chem*.,**1995**, 99, 3100.

[11] A.D.Becke *J.Chem.phys*.,**1993**, 98, 5652.

[12] M.J.Frisch et al.Gaussian, Inc., Wallingford CT,**2004**.

[13] C.Lee, W.Yang and R.G.Parr.*phys.Rev*., **1988,**B37,pp.784-789.

[14]N.Sundaraganesan;H.Saleem;S.Mohan;M.Ramalingam.*Spectrochim.Acta*.,**2005,** A61,385.

[15] N.Sundarganesan, S.Ilakimani, H.Saleem, P.M.Wojaechiwsju, D.Michalska, *Spectrochim acta.*, **2005,** A61, 3001.

[16] J.A.Pople, H.B.Schlegel, R.Krishnan, D.J.Defrees, J.S.Binkley, M.J.frisch, R.A.Whiteside R.J.Hout, and W.J.Hehre, *Int.J.Quantum Symp*., **1981,** 15, 269.

[17] J.A.pople, AP.Scott, M.W.Wong and L.Radom, *Isr.J.Chem*.,**1993,** 33, 350.

[18] MH Jamroz, Vibrational Energy Distribution Analysis, VEDA 4 Program, Warsaul.,**2004**.

[19] GrigorityA.Zhurko.Denis.A.zhurko, **2004,** chemcraft program.Academic version 1.5.,

[20] Y.Nawala.N.Terao, T.Terazono, k.Igasa, Y.Yutanj and K.Ochi, *Acta Cryst.C* **1987,** 43, 2462.

[21] http://chemcraft.com.

[22] D. Michalska, Raint Program, Wroclaw University of Technology,**2003.**

[23] D.Michalska and R.Wysokinski, *Chem.Phys.Lett*,**2005**, 403,217.

[24] G.Socrates,*Infrared characteristic group frequencies*, John wiley and sons,New **York,** 1980**.**

[25] Parker F S, Kirchenbaum, *Spectrochim Acta*.,**1960,** 16, 910

[26] N. Sundaraganesan, C. Meganathan, H. Saleem, B. D. Joshua , *Spectrochim Acta Part* A, **2007**, 68, 625.

[27] R.M.Silverstein, G.Clayton Bassler, T.C.Morrill, Spectroscopic identification of Organic compounds*,* 4E, John Willey,New York,**1981**.

.[28] S.E.Wberly et al *Anal, Chem*.,**1960**, 32, 217

[29] J.H.S Green, and D.J.Harrison, *Spectrochim Acta*, **1973**, 29A ,293

[30] R.Tripati, *Indian J.pure Appl.Phys*,**1973**, 11,277

[31] L.Bellamy," The infrared spectra of complex molecules", 3rd edition, Chapman Hall Ltd, London, Halted Wiley, New York **1975**

[32] C.H.Kline Jr and J.Turkerich, *J.Chem.Phys*,**1944**, 12,300

[33] C.W.Young, R.B.Durall and N.Wright, *Anal.Chem.,***1951**, 23, 709.

[34] B.R.D.B. Praser and W.C.Price, Pro.Roy. Soc., B141,66,1953 and *Nature*., **1952,** 170, 491.

[35] C.Pandian.M.phil Thesis (DDE), Annamalai University, **2009**.

_____

[36] A.Teimouri, A.N.Chermahini and M.Emami *ARIVOC*, **2008,** 12, 187

[37] R.A.Yadav, I.S.singh,*Indian J.Pure appl.Phys*., **1985**, 23, 626.

[38] W.Zierkiewiez, D.Michalska, Th.zeegers-Huyskens*, j.phys.chem*.,**2000**, 104A, 11685.

[39]] N.Sundaraganesan, C.Meganathan, B.Domoinic Joshua, P.Mani, A.Jayaprakash, *spectrochim.Acta,* **2008**, 71A, 1134.

[40] E.F.Mooney, *Spectrochim.Acta.,* **1964**, 20, 1343.

[41] J.E.Burch, E.Gerrard, M.Goldstein, E.F.Mooney, D.E.Pratt, H.A.Willis,*Spectrochim Acta.,***1963,** 19, 889.

[42] V.Krishnakumar, N.Surumbarkuzhali, S.Muthunatesan, *Spectrochim Acta*., **2009,** 71A, 1810.

[44] M.A.Palofox,*Int.J.Quant.Chem*.,**2000,** 77, 661

[45]N.Sundaraganesan,G.Elango,C.Meganathan,B.karthikeyan,M.Kurt,Molecular simulation, **2009,** 35, 705.

[46]G .Varsanyi   Assignments   for   vibrational   spectra   of   seven   hundred   benzene Derivatives,**1994,** vols 1 and 2 Adam Hilger.

[47] M. A. Palafox, *Int J Quantum Chem*,**2000,** 77,pp.661-684.

[48] T.vijayakumar,I.H.Joe,C.P.R.Nair,V.S.Jaykumar,*Chemical physics*.,**2008,** 343,83.

[49] Parthasarathi, M Elango, J Padmanabhan, V Subramanian, D R Roy , U Sarkar & K Chattaraj, *Indian j Chem*.,**2004,** 45A, 125.

[50] D. A.Prystupa, A.Anderson , B. H. Torrie *J Raman spectroscopy*.,**1994,** 25, 182.